Electric Vehicle Charging Station Placement Method for Urban Areas

Qiushi Cui, Member, IEEE, Yang Weng, Member, IEEE, and Chin-Woo Tan, Member, IEEE

Abstract—For accommodating more electric vehicles (EVs) to battle against fossil fuel emission, the problem of charging station placement is inevitable and could be costly if done improperly. Some researches consider a general setup, using conditions such as driving ranges for planning. However, most of the EV growths in the next decades will happen in the urban area, where driving ranges is not the biggest concern. For such a need, we consider several practical aspects of urban systems, such as voltage regulation cost and protection device upgrade resulting from the large integration of EVs. Notably, our diversified objective can reveal the trade-off between different factors in different cities worldwide. To understand the global optimum of largescale analysis, we studied each feature to preserve the problem convexity. Our sensitivity analysis before and after convexification shows that our approach is not only universally applicable but also has a small approximation error for prioritizing the most urgent constraint in a specific setup. Finally, numerical results demonstrate the trade-off, the relationship between different factors and the global objective, and the small approximation error. A unique observation in this study shows the importance of incorporating the protection device upgrade in urban system planning on charging stations.

Index Terms-Electric vehicle charging station, distribution grid, convexification, protective devices upgrade.

#### Nomenclature

NOMENCLATURE
The inflation rate, $(n = 1, \dots 6)$ .
The discount rate, $(n = 1, \dots 6)$ .
Expanded line capacity at node i, in kVA.
Expanded substation capacity at node i, in kVA.
Voltage deviation from nominal voltage $V_{nom}$ at node
i, in p.u.
Set of nodes in the distribution networks.
The probability that the $n^{th}\ {\rm EV}$ owner will choose
the $i^{th}$ charging station of service provider $k$ .
Set of branches in the distribution networks.
The protective device capacity.
$c_{dc}^{st},c_{dc}^{uninst},c_{dc}^{main}$ The acquisition, installing, unin-
stalling, and maintenance costs respectively, for the
protective device of type $d$ capacity $c$ , in $\$$ .
Fixed cost to build a new station at node $i$ .
Fixed cost to add an extra spot in the existing
charging station at node $i$ .
Line cost at node $i$ , in $\frac{kVA \cdot km}{k}$ .

dThe protective device type. Qiushi Cui and Yang Weng are with the Department of Electrical and Computer Engineering, Arizona State University, Tempe, AZ, 85281 USA

(e-mail: qiushi.cui@asu.edu; yang.weng@@asu.edu). Chin-Woo Tan is with

Stanford University, Stanford, CA, 94305 USA (e-mail: tancw@stanford.edu).

square, in  $\$/p.u.^2$ .

 $(n=1,\cdots 5).$ 

Substation expansion cost at node i, in kW.

Voltage regulation cost coefficient per p.u. voltage

The economic coefficient at node i at the  $t^{th}$  year,

 $c_{4,i}$ 

 $c_5$ 

 $c_{n,i,t}$ 

 $D_{i,k}$ The average charging demand that each spot satisfies from service provider k at bus node i, in MW.

Maximum current limitation at branch i, in Amp.  $I_{max,j}$ Length of the distribution line expansion required for a new charging station at node i.

Total number of branches in the distribution netmworks.

Total number of nodes in the distribution networks. The number of EVs at downstream of line l.

Original line capacity at node i, in kVA. The power of the integrated EV, in W.  $P_{sur}$ The substation surplus capacity, in MW.

 $R_d$ The number of ranges of the continuous current of protective device type d.

SThe minimum power demand in a certain area, aggregated by zip code, in MW.

TThe total life of the project. The year of the project.  $V_i$ 

Voltage at node i, in Volt.  $V_{max,i}$ Maximum voltage limitation at node i, in Volt.

Minimum voltage limitation at node i, in Volt.  $V_{min,i}$ Binary variable denoting charging station location at  $x_i$ 

node i.

Binary variable,  $x_{ldc} = 1$  when line l is determined  $x_{ldc}$ to upgrade its protective device to type d capacity c.

Binary variable,  $x_{ldc}^{base} = 1$  when line l initially has  $x_{ldc}^{base}$ the protective device of type d capacity c.

Number of new charging spots to be installed in the  $y_i$ station of node i.

Binary variable, equal to zero when the element (d, c)

of the matrix A is negative.

#### I. INTRODUCTION

NDER the Paris agreement signed in 2016, the model of a sustainable urban city - Singapore, pledged to cut emissions intensity by 36% below 2005 levels by 2030 [1]. To meet the commitment, emissions reduction worldwide in the transport sector is crucial, and large-scale electric vehicle (EV) adoption in the future is, therefore, utmost essential to Singapore and many other cities/countries. For example, Singapore took several important steps in this direction such as 1) an announcement of a new Vehicular Emissions Scheme [2] and 2) the launch of the electric vehicle car-sharing program [3], etc. However, one of the major barriers to successful adoption of EVs at a large scale is the limited number of available charging stations. Thus, it is important to properly deploy EV charging infrastructure to enhance the adoption of EVs efficiently.

EV charging station placement has therefore been an active research area for intercity and urban infrastructure planning.

In freeway charging infrastructure planning, [4] tackles the EV charging station placement problem in a simple round freeway, whereas [5] proposes a capacitated-flow refueling location model to capture PEV charging demands in a more complicated meshed transport network. However, both papers share the similarity of considering the driving range in the freeway. In contrast, the driving range constraints are not prominent in the urban area charging infrastructure planning since the charging stations are easily accessible, therefore, researchers have considered various aspects dedicated for urban area charging station placement. For example, [6] manages to find the optimal way to recharge electric buses with long continuous service hours under two scenarios: with and without limited batteries. However, it is applicable only to public bus systems. [7] considers urban traffic circulations and hourly load change of private EVs, but it ignores the geographical land and labor cost variation that are of high importance in urban areas.

If zooming in on the specific techniques deployed and the realistic factors considered, the problem under study can be examined in various technical aspects. For example, [8] includes the annual cost of battery swapping, and [9] considers the vehicle-to-grid technology. Furthermore, researchers and engineers explore many realistic factors such as investment and energy losses [10], quality of service [11], service radius [12], etc. The work in [13] considers the EV integration impact on the grid. In fact, when the load profiles change, the electrical demand at particular points can exceed the rated value of the local T&D infrastructure. A study in the U.S. has put the value of deferring network upgrade work at approximately \$650/kW for transmission and \$1,050/kW for distribution networks [14]. Besides the techniques in the previously mentioned papers, studies focusing on the infrastructure upgrade, therefore, seems necessary under large-scale EV integration. Some papers discuss infrastructure upgrade. For example, [9] takes into account the loading limits of the distribution transformer and distribution lines; while [15] considers minimizing the voltage deviation cost. However, realistic factors like the upgrade of protective devices and its effect on the overall planning are not addressed in the context of EV charging station integration in the past.

The aforementioned urban planning and technical issues are mainly formulated as optimization problems. Based on the nature of the equations involved, these optimization problems contain linear programming as well as the nonlinear programming problems [9], [10]. Based on the permissible values of the decision variables, integer programming, and real-valued programming usually, exist in the same EV charging station problem [16]. Based on the number of objective functions, both single-objective [5] and multi-objective [10], [17] problems are proposed by researchers. Variously, the optimization problems are sometimes considered on a game theoretical framework in [11], [18]. Solutions to these optimization problems include greedy algorithm [6], [16], genetic algorithm [9], interior point method [12], gradient methods [11], etc. However, these solutions do not consider the convexification of the constraints. Consequently, they are unable to guarantee a global optimum.

The contributions of this paper include three points. Firstly, this paper quantifies the protection device upgrade cost with step functions and integrates the protection cost into the objective function of the EV charging station placement. The effect of protection and voltage regulation upgrade on the charging station placement is revealed. Secondly, the convexification preservation is realized in this optimization problem, at the same time, the global optimum is achieved and guaranteed. Thirdly, this paper suggests a comprehensive sensitivity analysis before and after the problem convexification. The sensitivity validation further indicates the applicability of the proposed method in different cities and countries.

The established optimization problem originates from the practical concerns within electrical and transportation networks. Its sensitivity is firstly analyzed, then the constraint convexification is conducted. Meanwhile, the sensitivity analvsis is re-evaluated after the problem convexification to see if it still holds. In the end, the proposed objective function along with its constraints will provide the results for the EV charging station planning, which satisfies the economic requirements that both networks request. The outline of the paper comes as follows: Section II elaborates on the mathematical formulation of the problem under study. Based on the proposed formulas, Section III suggests a way of convexifying the proposed realistic constraints in the objective function. Section IV demonstrates the numerical results as well as sensitivity analysis after convexification in small and large scale systems respectively. Furthermore, the discussions on the geographical effect and the importance of protection cost are presented in Section V. The conclusions are in Section VI.

#### II. PROBLEM FORMULATION

Fig. 1 shows the flowchart of the proposed EV charging station placement method. It considers the integrated electrical and transportation networks as well as their associated infrastructure costs. Therefore, the costs related to distribution expansion, voltage regulation, protective device upgrade, and EV station construction are incorporated in the objective function. This study is assumed to be conducted for urban cities and large scale of EV integration in the future. Since a great amount of stations has to be installed in this circumstance, the EV charging station integration point could be at any bus along the distribution feeder as long as the operation constraints permit. In this section, the objective function and constraints are first formulated and then explained in details. Afterwards, the sensitivity analysis is provided from a mathematical angle.

#### A. Objective Function and Constraints

The objective function minimizes the total cost among the costs of charging stations, distribution network expansion, voltage regulation, and protection device upgrade. It is formulated as a mixed-integer nonlinear optimization problem:

$$\underset{x_{i}, y_{i}}{\text{minimize}} \quad C_{sta} + C_{dis} + C_{vr} + C_{prot} \tag{1}$$

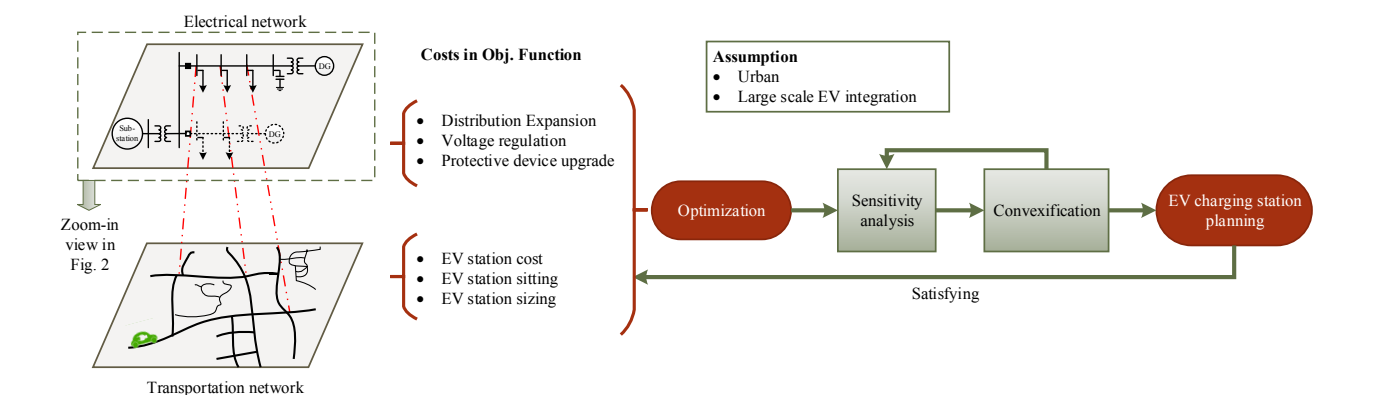


Fig. 1. Flowchart of the proposed EV charging station placement method.

subject to

$$x_i \in \{0,1\}, i \in \Phi,$$
 (2a)

$$y_i \in \mathbb{Z}^+, \ i \in \Phi,$$
 (2b)

$$\sum_{i \in \Phi} g(y_i) \ge S, \ i \in \Phi, \tag{2c}$$

$$f(V_i, \delta_i, P_i, Q_i) = 0, \ i \in \Phi, \tag{2d}$$

$$0 \le |I_i| \le I_{max,i}, j \in \Psi, \tag{2e}$$

$$V_{min,i} \le |V_i| \le V_{max,i}, \ i \in \Phi, \tag{2f}$$

$$C_{sta} + C_{dis} + C_{vr} + C_{prot} \le C_{budget},$$
 (2g)

where

$$C_{sta} = \sum_{i \in \Phi} (c_{1,i} x_i + c_{2,i} y_i), \tag{3}$$

$$C_{dis} = \sum_{i \in \Phi} (c_{3,i} l_i (P_{0,i}^{line} + \Delta P_i^{line})) + c_{4,i} h(\Delta P_i^{sub}), \quad (4)$$

$$C_{vr} = c_5 \sum_{i \in \Phi} \Delta V_i^2, \tag{5}$$

$$C_{prot} = C_{acq} + C_{inst} + C_{uninst} + C_{main}. (6)$$

The definition of the notations is in the Nomenclature.

The formulated objective function deals with the planning, specifically, the sitting and sizing of the charging stations. It is, therefore, the distribution system operator (DSO) who solves the optimization problem. In the deregulated electricity markets in the States (such as California ISO, PJM, and ERCOT), the market coordinator of the distribution networks calculate the locational marginal prices (LMPs) at each node. Then the wholesale market sells the electricity to the charging stations that are run by the EV charging service providers at the LMPs. The service providers provide charging service at retail charging prices accordingly. For one thing, the DSO plans the charging station placement to minimize its grid operation cost and EV infrastructure investment using (1). For another thing, the service providers always attempt to maximize the profit once the EV infrastructure is built.

In the remaining part of Section II, the objective function and constraints are explained first, then the problem sensitivity is analyzed from the mathematical perspective.

#### B. Explanations of the Objective Function

The objective function aims to minimize the total cost associated with four aspects in (1). They are visualized in Fig.

2, which is zoomed in from the electrical network in Fig. 1. There are four terms (also viewed as four constraints) in this objective function. They are related to different aspects of EV charging and network upgrade costs.

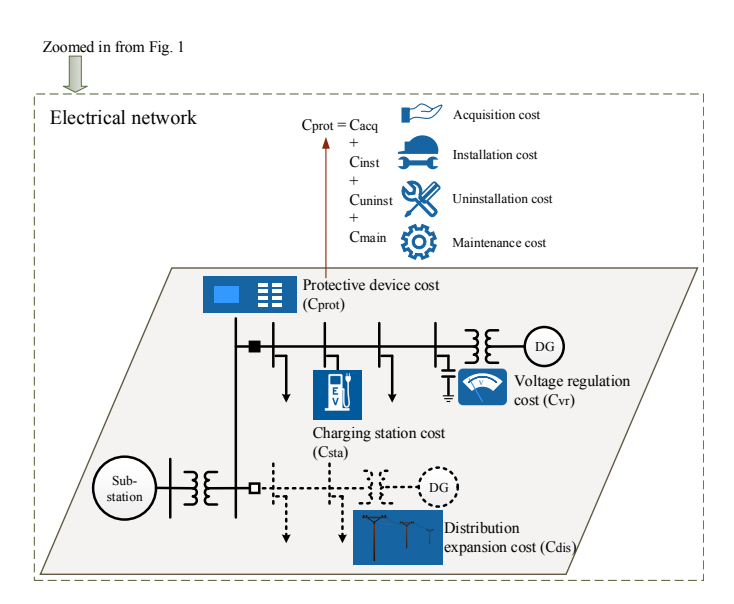


Fig. 2. Cost decomposition – Zoom-in of the electrical network.

The first term is the fixed cost of building a new station and of adding an extra spot in the existing charging station. The second one is related to the distribution line cost and the substation expansion cost. The distribution line cost is approximately proportional to the product of the line length and the total line capacity. Moreover, the total line capacity is the sum of the original line capacity and the expanded line capacity, where the latter can be estimated to be proportional to the number of new charging spots to be installed:

$$P_{0,i}^{line} + \Delta P_i^{line} = P_{0,i}^{line} + p_{ev}y_i, \quad i \in \Phi.$$
 (7)

The second term considers the distribution system expansion cost including substation capacity upgrade, branch capacity upgrade, branch expansion, etc. When a charging station location that can satisfy a certain area's charging demand is not directly accessible from the closest distribution network bus, an expansion of the existing distribution line, either in

MV or LV level, is needed to deliver power to this charging station. Also in the second term, an h function is employed to describe the net power increase according to the substation surplus capacity  $P_{sur}$ . The h function is defined as follows:

$$h(\Delta P_i^{sub}) = \begin{cases} 0, & \Delta P_i^{sub} < P_{sur}, \\ p_{ev} \sum_i y_i, & \Delta P_i^{sub} \ge P_{sur}. \end{cases}$$
(8)

The third term represents the equivalent cost resulting from the impact of EV charging stations on the distribution network voltage profile, where  $\Delta V_i = V_i - V_{i,ref}$ . [19] proposes a stochastic capacitor planning formulation for distribution systems. However, voltage regulation techniques in distribution systems include voltage regulation transformers, static var compensators, static synchronous compensators, and shunt capacitor banks, etc [20]. They can maintain voltage levels of load buses within an acceptable range. Since  $Q = V^2/X_c = \omega CV^2$ , the amount of reactive power compensation is proportional to the bus voltage. Therefore the square of voltage deviation from the reference voltage at each bus is employed to evaluate the voltage regulation related cost.

The fourth term is associated with the protection device upgrade due to the installation of EV charging stations. The protection cost decomposition is shown at the top of Fig. 2. It is assumed that the acquisition, installation, uninstallation, and maintenance costs are constant at each current range. The capacity c is an integer, denoting a specific numbered capacity range up to  $R_d$ , for the protective device with type d. For example,  $c=1,\cdots,5$  for the fuses, according to Table VIII. The matrix A indicates the total number of devices to be installed [21]:

$$A(d,c) = \sum_{l=1}^{m} (x_{ldc} - x_{ldc}^{base}).$$
 (9)

Therefore, we have:

$$C_{acq} = \sum_{d=1}^{4} \sum_{c=1}^{R_d} c_{dc}^{acq} \cdot z_{dc} \cdot A(d, c), \tag{10}$$

$$C_{inst} = \sum_{d=1}^{4} \sum_{c=1}^{R_d} \sum_{l=1}^{m} (c_{dc}^{inst} \cdot x_{ldc} \cdot (x_{ldc} - x_{ldc}^{base})), \quad (11)$$

$$C_{uninst} = \sum_{d=1}^{4} \sum_{c=1}^{R_d} \sum_{l=1}^{m} (c_{dc}^{uninst} \cdot x_{ldc}^{base} \cdot (x_{ldc} - x_{ldc}^{base})),$$

$$(12)$$

$$C_{main} = \sum_{d=1}^{4} \sum_{c=1}^{R_d} \sum_{l=1}^{m} (c_{dc}^{main} \cdot x_{ldc}), \tag{13}$$

where

$$x_{ldc} = \begin{cases} 1, & I_0 + \Delta I_{ld} = I_0 + n_{dn\_ev}^l \cdot I_{ev}^0 \in c, \\ 0, & \text{otherwise.} \end{cases}$$
 (14)

On one hand, the proposed mathematical model considers the fuses, reclosers, overcurrent relays, and directional overcurrent relays with synchronized recloser function in this paper. Extra devices can be added depending on the specific cases. On the other hand, the value selection of each device capacity is according to the realistic device operating ranges. Different costs of the protective devices can be found in

Appendix A. We assume there is no relocation during device upgrade since the original placement of the recloser was very likely determined by the reach of the feeder relays. Replacement of the recloser with directionality function is preferred in practice [22].

#### C. Explanations of the Constraints

- 1) Optimization variables in (2a) and (2b):  $x_i$  is a binary variable that indicates the availability of the charging station at bus node i, and  $y_i$  is an integer variable that shows the number of charging spots at bus node i.
- 2) Charging serviceability constraint in (2c): the charging station serviceability needs to be higher or equal to the minimum power demand S in a certain area. The charging serviceability is the summation of the serviceability function  $g(y_i)$  over all charging locations. To simplify the problem, we use

$$g(y_i) = D_{i,k} y_i, (15)$$

to represent the charging demand. We include in this paper the nested logit model [11] to predict and quantify the charging demand  $D_{i,k}$ . The social welfare behind  $D_{i,k}$  contains the influence from the EV owner preference, charging prices, road connections, traffic conditions and the number of EVs in that area. Details of the nested logit model and how it quantify the social welfare is given in Appendix B.

- 3) Power flow constraints in (2d): the integration of EVs and locally distributed generations should respect the constraints of the electric network. The function f denotes the power flow equations.
- 4) Line current constraint in (2e): the current flowing in each line should not exceed the maximum rated current of the line.
- 5) Voltage limits in (2f): for the operation safety, the voltage range of  $0.95 \sim 1.05$  is recommended.
- 6) Budget limits in (2g): for the generality of the proposed method, this constraint can be estimated ahead of the overall optimization and planning. Concisely, the budget constraint depends on the regional EV flow that EV supply equipment can host in each planning stage, along with other system upgrade costs. This constraint can be ignored based on the requirement of different utilities.

#### D. Sensitivity Analysis of the Problem

In order to analyze the sensitivity of each constraint in the objective function (1), the comparison is made in (3)-(6). Specifically,  $C_{sta}$  in (3) can be rearranged into  $c_{1,i} \sum_{i \in \Phi} x_i + c_{2,i} \sum_{i \in \Phi} y_i$ ; while  $C_{dis}$  in (4) can be decomposed into the following format using (7)-(8) when  $\Delta P_i^{sub} \geq P_{sur}$ :

$$C_{dis} = \sum_{i \in \Phi} c_{3,i} l_i P_{0,i}^{line} + (c_{3,i} l_i p_{ev} + c_{4,i} p_{ev}) \sum_{i \in \Phi} y_i.$$
 (16)

Now each term in the objective function seems comparable: Constraint (3): In  $C_{sta}$ , generally, the number of the stations is smaller than that of the spots, and the cost of building a

station is higher than that of a spot. Therefore,  $x_i$  is smaller than  $y_i$ , whereas  $c_{1,i}$  is larger than  $c_{2,i}$ .

Constraint (4): Between  $C_{sta}$  and  $C_{dis}$ , the values associated with  $\sum_{i\in\Phi}y_i$  depends on their coefficient  $c_{2,i}$  and  $(c_{3,i}l_ip_{ev}+c_{4,i}p_{ev})$ . Furthermore,  $C_{dis}$  has a relatively constant part  $\sum_{i\in\Phi}c_{3,i}l_iP_{0,i}^{line}$  whereas  $C_{sta}$  has the sub-term  $c_{1,i}\sum_{i\in\Phi}x_i$  that relies on the optimized number of stations.

Constraint (5):  $C_{vr}$  grows relatively faster than other terms when  $c_5$  is remarkable due to the square term. Meanwhile, the  $\Delta V_i^2$  part in (5) indicates a strong relevance with placements that boost up bus voltages.

Constraint (6): The sub-terms in  $C_{prot}$  does not increase as fast as the ones with  $\sum_{i\in\Phi}y_i$ , and they mainly depend on the current-cost relationship as assumed in Section II-B. This means that the EV charging station placements resulting in high current absorption would increase the cost in this term.

#### E. Variation of the Economic Parameters

The variation of economic parameters is considered in this subsection. Factors like the time value and the uncertainty of the cost cannot be ignored sometimes since some costs in the objective function are related to an early stage of the project and some are postponed to a later stage. Consequently, the levelized cost coefficients are proposed. The idea comes from the levelized cost of energy, which is extensively studied in systemically analyzing comparable projects and establishing renewable energy policy [23]–[25]. The four terms in (1) are levelized as follows:

$$C_{sta}^{lev} = \sum_{i \in \Phi} \left(\sum_{t=0}^{T} c_{1,i,t} \frac{(1+\alpha_1)^t}{(1+\beta_1)^t} x_i + \sum_{t=0}^{T} c_{2,i,t} \frac{(1+\alpha_2)^t}{(1+\beta_2)^t} y_i\right),\tag{17}$$

$$C_{dis}^{lev} = \sum_{i \in \Phi} \left( \sum_{t=0}^{T} c_{3,i,t} \frac{(1+\alpha_3)^t}{(1+\beta_3)^t} l_i (P_{0,i}^{line} + \Delta P_i^{line}) \right)$$
(18)

$$+\sum_{t=0}^{T} c_{4,i,t} \frac{(1+\alpha_4)^t}{(1+\beta_4)^t} h(\Delta P_i^{sub}), \tag{19}$$

$$C_{vr}^{lev} = \sum_{t=0}^{T} c_{5,i,t} \frac{(1+\alpha_5)^t}{(1+\beta_5)^t} \sum_{i \in \Phi} \Delta V_i^2,$$
 (20)

$$C_{prot}^{lev} = \sum_{t=0}^{T} c_{6,i,t} \frac{(1+\alpha_6)^t}{(1+\beta_6)^t} (C_{acq} + C_{inst} + C_{uninst} + C_{main}),$$
(21)

where t is the year of the project, T is the total life of the project,  $\alpha_n(n=1,\cdots 6)$  is the inflation rate,  $\beta_n(n=1,\cdots 6)$  is the discount rate. The inflation rate denotes the increase in the price index. The discount rate originates from the net present value theory and can be understood as the return that could be earned in alternative investments.

The equation (1) can now be rewritten as

$$\underset{x_i, y_i}{\text{minimize}} \quad C_{sta}^{lev} + C_{dis}^{lev} + C_{vr}^{lev} + C_{prot}^{lev}. \tag{22}$$

#### III. PROBLEM CONVEXIFICATION

Following the sensitivity analysis of the previous section, this section discusses the way of convexifying the nonlinear terms in the objective function. Furthermore, the approximation error is discussed in the second part. By convexifying the optimization constraints, we can achieve (1) the guarantee of a global minimum solution in both small and large electric systems, and (2) a decreased computational time. The tradeoff is that the convex preservation contributes to some errors during optimization. More details regarding the trade-off can be found in Section IV.

#### A. Convexify the Problem

The linearization of the AC power flow in constraint (2) is depicted in Appendix C. This paper does not focus on AC power flow linearization. For the reference of the audience, other relevant methods on AC power flow linearization including the DistFlow and second-order conic relaxation can be found in [26], [27]. In addition, other constraints in (2) are linear. Therefore, greater emphasis is to be placed on the constraints from the objective function.

- 1) Constraint (3): It is a linear combination of the number of stations and the number of spots. Therefore it is convex.
- 2) Constraint (4): The first part of this constraint is linear, whereas the second part of this constraint is not linear as indicated in (8). However, the piece-wise linear function (8) becomes linear when the substation surplus capacity (assuming to be 1 MW in this paper) is exceeded. It actually means that as long as there are more than  $1MW/0.044MW \approx 23$  spots to be built downstream from the entire substation, this constraint is linear.
- 3) Constraint (5): In this constraint, the optimization variable  $x_i$  is linearly related to the net active power injection  $P_i$  at bus i in power flow calculation:

In this constraint, the variable  $V_i$  is a nonlinear function of the optimization variable  $x_i$ , which is linearly related to the net active power injection  $P_i$  at bus i in power flow calculation:

$$P_{i,inj} = P_{i,gen} - P_{i,load} - x_i p_{ev}, \ i \in \Phi, \tag{23}$$

but the variable  $V_i$  is a nonlinear function of the optimization variable  $x_i$ . Utilizing the AC power flow linearization technique as elaborated in Appendix C, we can easily establish the linear relationship between the optimization variable x and the non-slack bus voltage  $V_N$ . It is convex and a global optimum is guaranteed.

4) Constraint (6): Given the assumption of this constraint, the protection cost is actually a summation of four piece-wise step functions including the costs of acquisition, installation, uninstallation, and maintenance. Its curve is plotted in Fig. 3. To linearize the step functions, these step functions in Fig. 3 are approximated by three linear lines (the dash-dot lines in blue) using the linear curve-fitting algorithm.

#### B. Convexification Error Analysis

The convexification error analysis is conducted in the same order as in the previous section. The convexification of the AC power flow in constraint (2) uses the same linearization technique like the one in constraint (5) from the objective function. The following convexification errors are elaborated.

 Constraint (3): No approximation error associated with this constraint since it is a linear constraint itself.

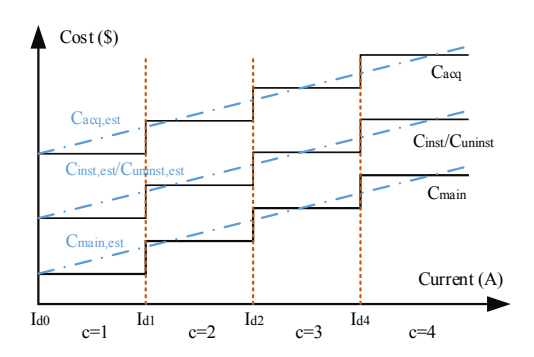


Fig. 3. Cost functions of protective devices and their estimated and linearized functions. Assume there are four levels of capacity for the device type d.

- Constraint (4): The largest approximation error occurs at the turning point where 23 spots are planned but substation expansion is not yet required. However, if the number of spots to be built is larger than 23, there will be no error associated with this constraint.
- Constraint (5): The approximation error originates from the quadratic term that is neglected in the derivation of the voltage-power equation, the details of which can be found in Appendix C. The error in complex power originates from the high order series of the following Taylor expansion. If we neglect high order terms and defining  $V=1-\Delta V$ , a linear form is obtained when  $||\Delta V||<1$ :

$$\frac{1}{V} = \frac{1}{1 - \Delta V} = \sum_{n=0}^{+\infty} (\Delta V)^n \approx 1 + \Delta V = 2 - V. \tag{24}$$

The error in percentage for the approximation is calculated by defining a function  $\Psi(V) = 100 \cdot ||(1/V) - (2 - V)||$ .  $L_2$ -norm is employed here.

• Constraint (6): To simplify this constraint, a best-fitting straight line for each protective device is obtained based on realistic costs (refer to Appendix A for details) and R-squared values as shown in Table I. The closer the R-squared value is to 1.0, the better the fit of the regression line. We see that all four types of devices' R values are above 0.75, which fairly represents the realistic device costs.

TABLE I
BEST TREND-LINE ON ESTIMATING THE PROTECTIVE DEVICE COSTS
USING THE DATA IN APPENDIX A.

Device type	Cost function (c) w.r.t. current (I)	$R^2$
Fuse	c = 3.771I + 548.26	0.775
Recloser	c = 16.381I + 18219	0.797
Overcurrent relay	c = 2.040I + 4515.9	0.756
DORSR	c = 2.040I + 6515.9	0.756

#### C. Sensitivity Analysis

The errors according to the above analysis are small and have little influence on the sensitivity of the problem. For example, the constraint (3) is linear by itself. The constraint (4) is also linear when below or above a certain number of charging spots. The constraint (5) has a maximum error of 0.26% in the  $\Psi(V)$  equation if the deployed voltage regulator regulates the bus voltage between 0.95 and 1.05.

The constraint (6) does not present a large cost change among each two adjacent current ranges based on the realistic data in Appendix A. Therefore the protective cost can be assumed as a constant when the continuous current setting is within a range of operating currents [21]. In the next section, the numerical results will validate the problem sensitivity in various aspects.

#### D. Feasibility Analysis

As an important part of this optimization problem, the linearization of the power flow equations has made this problem an NP problem. It also contributes a big portion of the approximation error. Mathematically, it might result in a global solution outside of the feasible region of the main optimization problem. Therefore, by revisiting the constraint (2d), we know that the power flow linearization establishes a linear relationship between the solution (it directly determines the power demand  $P_i, Q_i$ ) and the complex voltage. The error of the power flow linearization directly affects the objective function through constraint (5), which is the voltage regulation cost. During optimization, the solver searches for the optimal solution that minimizes the overall cost, consequently, the power flow linearization affects the solution and its errors.

To evaluate the feasibility of the solution, it is recommended to plug the solution back to the AC power flow and the main optimization problem as a validation. The solution evaluation comes in twofold. Firstly, if the solution is within the feasible region of the main optimization problem, no corrective action is required. Secondly, if the solution is within the infeasible region, we recommend using a weighted constraint violation metric to quantify the error. We formulate all the inequality constraints in (2) in the format of  $b_{i,min} \leq a_i(x) \leq b_{i,max}, i = 1, \cdots, r$ , where r is the number of constraints. Then for a solution  $x^*$  obtained from the convexified problem, the constraint violation metric  $V_c$  is defined as follows:

$$V_c = \sum_{i=1}^{r} [a_i(x^*) - b_{i,max}]_+ + \sum_{i=1}^{r} [b_{i,min} - a_i(x^*)]_+, \quad (25)$$

where the operator  $[\cdot]_+$  keeps the value inside the bracket unchanged when it is non-negative, and output zero when it is negative. The weight of each constraint is at the utility or DSO's discretion. To simplify this problem, we assume each term has a weight of 1.

#### IV. NUMERICAL RESULTS

After discussing the way of convexifying the constraints in the objective function, this section demonstrates the effect of each constraint from the objective function on the overall problem using realistic data. After introducing the cost parameters and the systems under study, we investigate the sensitivity of the formulated problem from small to large systems.

#### A. Cost Parameters

The fixed costs for each PEV charging station is assumed to be  $c_{1,i}=163,000\,(\$)$  [5]. The land use costs are  $407\,\$/\mathrm{m}^2$  and adding one extra charging spot requires  $20\,\mathrm{m}^2$  land. The per-unit purchase cost for one charging spot is  $23,500\,\$$  [28]. Thus we have  $c_{2,i}=407\times20$  +

23,500=31,640 (\$). The distribution line cost is assumed to be  $c_{3,i}=120$  (\$/(kVA·km)) [29]. The substation expansion cost is assumed to be  $c_{4,i}=788$  (\$/kVA) [10].

The charging demand,  $D_{i,k}$ , that each spot satisfies, follows the constraint (2c) and the nested logit model, the coefficients of which are estimated from the preference survey data [30]. We assume the distribution feeder has 1 MVA surplus substation capacity which can be utilized by charging station. The rated charging power for each charging spot is  $44 \,\mathrm{kW}$  [5]. The voltage regulation coefficient  $c_5$  is assumed to be 50,000 (\$) according to [31], given the base power of  $100 \,\mathrm{MVA}$ . Per car, the charging current is assumed to be  $44 \,\mathrm{kW} / \sqrt{3} / 12.5 \,\mathrm{kV} = 2 \,\mathrm{A}$ .

#### B. Numerical Results of a Toy Example

This subsection demonstrates the station distribution of the entire system upon applying the constraints in an IEEE 4-bus small toy example then draws some interesting observations from this toy example. The results on large systems are presented in the next subsection.

The toy example is based on a modified IEEE 4-bus system as shown in Fig. 4. Besides the parameters in the previous subsection, an overcurrent relay is assumed to be installed next to B2 and a fuse next to B3. Meanwhile, B2 and B3 are also the only buses where an EV charging station can be built. Assuming also there are about 85 EVs per hour require charging services in the area under study and there is no limit for each charging spot. The charging demand is assumed to be  $(24 \, h \times 60 \, min/h)/(42 \, min \times 0.5) = 68 \, (vehicles/day)^1$  in this toy example. Therefore, we will have the total charging station spots of  $85 \times 24/68 = 30$ .

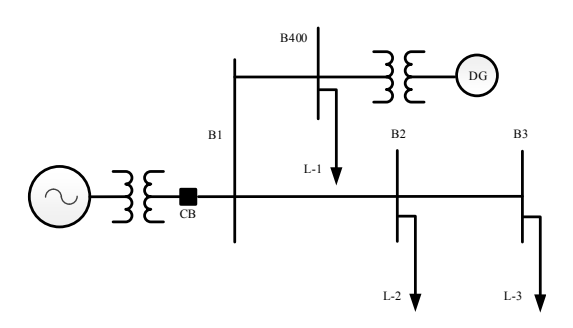


Fig. 4. IEEE 4-bus distribution system.

The placement results are presented by adding one constraint item after another to clearly observe the sensitivity of each constraint. Since there are many possible types of permutation of adding the four constraints, we have selected the constraint incremental procedure that best illustrates the nature of each constraint as shown in Table II. The following items illustrate the consequences in four representative scenarios:

1) The Constraint Added:  $C_{sta}$ : When there is only one constraint of charging station cost, the objective function attempts to build less number of stations for reducing the total cost as shown in (3). Since no spot limitation is assumed in

TABLE II
EV CHARGING STATION PLACEMENT RESULTS OF THE TOY EXAMPLE BY
ADDING THE CONSTRAINTS INCREMENTALLY.

Constraint	EV numbers at B2 & B3	$C_{total}(\$)$
$C_{sta}$	(0, 30) or (30, 0)	949, 200
$C_{sta} + C_{dis}$	(0,30) or $(30,0)$	2, 152, 360
$C_{sta} + C_{dis} + C_{vr}$	(0, 30)	2,160,360
$C_{sta} + C_{dis} + C_{vr} + C_{prot}$	(30,0)	2, 195, 210

this example, the optimal placements are a) no station built near B2 and 30 spots built near B3, or b) no station built near B3 and 30 spots built near B2. They are noted as (0,30), (30,0).

- 2) The Constraint Added:  $C_{sta} + C_{dis}$ : When the constraint of distribution system expansion is included, the EV placement is not changed. The reason for that is the constraint of  $C_{dis}$  depends on  $\sum y_i$  the total number of spots, which adds more cost but does not alter the placements within the buses for station installation. It is more economical to build fewer stations since the cost is saved by building one charging station as long as the capacity of the station is not violated.
- 3) The Constraint Added:  $C_{sta} + C_{dis} + C_{vr}$ : Now the voltage regulation constraint is also added to the objective function. It plays an influential role in favor of the placement that causes less voltage deviation. The resulting placement of (0,30) indicates that we have the minimum voltage violation by placing all the EVs at bus 3. To be noticed that voltage regulation cost might overwhelm other costs.
- 4) The Constraint Added:  $C_{sta} + C_{dis} + C_{vr} + C_{prot}$ : With the last constraint from a protection upgrade perspective, the optimal placement becomes (30,0). With the existence of this constraint, the placement moves from the end of the feeder towards the substation due to the characteristics associated with protective device upgrade: (a) the overcurrent relay (OC) relay upgrade at branch 1-2 (1 and 2 are the from and to buses respectively) is inevitable; (b) if all of the EV spots are placed at the end of the feeder, more protective devices are required to be upgraded along the feeder, and in this case, case 2 costs less since protective devices at branch 2-3 do not require an upgrade. Additionally, the land cost coefficients can overwhelm the voltage regulation cost and the protection cost, if the land cost in the urban area is expensive.

#### C. Numerical Results on a Large System

This subsection reveals the sensitivity analysis after convexification preservation on large systems. The benefits of problem convexification are first discussed. To observe the placement results, the optimization variables are evaluated. Subsequently, the cost analysis is added to validate the sensitivity. The deployed benchmark system in this section is the IEEE 123-bus distribution system (refer to Fig. 12 in Appendix D), and the costs and assumptions follow the ones in Section IV-A.

The urban traffic networks are built based on the Sioux Falls network [33], which has 24 transportation nodes and 76 links. To couple the electrical and distribution networks, we first adjust some node locations of the transportation network

 $<sup>^{1}</sup>$ The average charging time of an EV with empty battery is estimated as  $(200 \, \mathrm{km} \times 0.14 \, \mathrm{kWh/km})/(44 \, \mathrm{kW} \times 0.92) = 42 \, \mathrm{min} \, [32]$ 

while maintaining the same node connectivity, and then merge the two networks by assuming only the centroid transportation nodes (refer to Appendix E) are directly overlapping with selected electrical nodes. The coupling relationship of 13 centroid transportation nodes in the 123-bus distribution network is shown in Table III. The remaining electrical nodes that are not shown are assumed to be connected to the transportation network according to the nearest geographical locations.

TABLE III COUPLING RELATIONSHIP OF 13 CENTROID TRANSPORTATION NODES IN THE 123-BUS DISTRIBUTION NETWORK.

$T_1 \sim E_{110}$	$T_2 \sim E_{76}$	$T_4 \sim E_{101}$	$T_5 \sim E_{67}$	$T_{10} \sim E_{60}$
$T_{11} \sim E_{66}$	$T_{13} \sim E_{25}$	$T_{14} \sim E_{47}$	$T_{15} \sim E_{35}$	$T_{19} \sim E_{54}$
$T_{20} \sim E_{13}$	$T_{21} \sim E_1$	$T_{24} \sim E_{18}$		

Note: T: Transportation network. E: Electrical network.

1) The Benefits of Problem Convexification: Efforts are exerted on the convexification of the nonlinear constraints, the purpose of which is to guarantee a global optimum without jeopardizing the cost evaluation. Table IV illustrates the comparison between the scenario that convexifies all the constraints and the one does not.

TABLE IV

OPTIMIZATION RESULTS WITH AND WITHOUT CONSTRAINT CONVEXIFICATION IN THE 123-BUS SYSTEM.

Constraints	Without convexification	With convexification
Percent of cases that failed to find a global minimum	19.8% (50)	0.0% (0)
Average total cost in cases with a global minimum (\$)	$7.92 \times 10^7 \ (8)$	$7.96 \times 10^7 $ (11)
Average total cost in cases with a local minimum (\$)	$8.47 \times 10^7$ (3)	Unavailable
Computational time in cases with a global minimum (sec)	112.4 (8)	105.6 (11)
Computational time in cases with a local minimum (sec)	2, 115.7 (3)	Unavailable

Note: the numbers in the brackets denote the numbers of tests under the corresponding constraints.

Firstly, there are 23 cases tested in this section under different EV flows and station capacity limits in order to obtain the percent of cases that failed to find a global minimum. Since the initial points also affect whether the optimization objective function converges to a global minimum or not, 11 initial feasible points are, therefore, tested for each case to obtain the overall percentage of cases that failed to find a global minimum. As a result, 50 tests in total fail to converge to their corresponding global minimums. As is seen from Table IV,  $50/(23 \times 11) = 19.8\%$  of cases failed to find a global minimum due to the non-convexity constraints. Not surprisingly, all of the cases with convexified constraints successfully find the global minimum.

Secondly, the fact of convexifying the constraints does not affect much of the total cost. To maintain fair comparisons under the same EV demand and computational complexity, the average total cost and computational time have to be calculated

in the same case. In Table III, the demonstrated case is with the EV flow of 5,185 EVs/h and 25-spot limit per station. In this case, the solutions of 3 tests reach local minimums, and 8 tests reach global minimums. The total costs without and with convexification are calculated using equation (1) and averaged over their corresponding numbers of tests. Furthermore, in order to demonstrate the system-level performance after accumulating all errors due to convexification, Fig. 5 is presented here. The error is defined as the cost difference with and without convexification divided by the cost without convexification. As shown in Fig. 5, the total cost increases in the early stage when the EV flow is low since the optimization constraints force the charging stations to be built at high costs. At a later stage when the EV flow rises the overall cost reduces because fewer stations are built – more spots can be installed in the same station where the costs are low. Similar results are obtained in [5]. More importantly, the highest error is accumulated but does not exceed 4.4% as the number of EVs per hour increases. The mean error value in Fig. 5 is computed as 1.54%, therefore, the influence due to error accumulation on the system-level performance is limited.

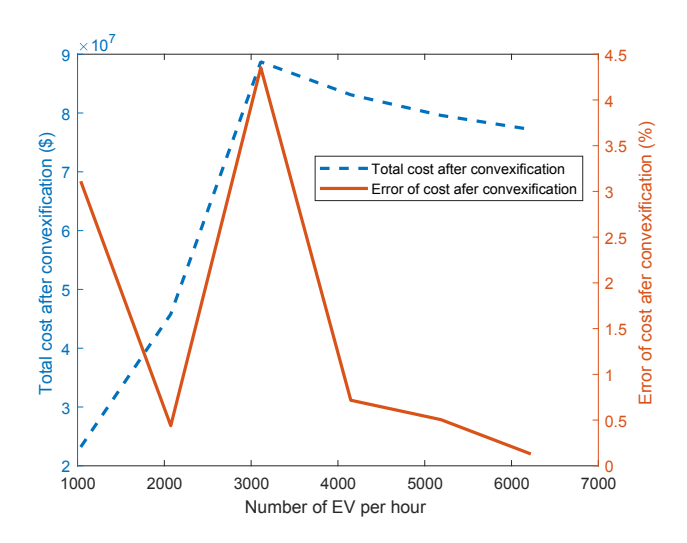


Fig. 5. The system-level performance after accumulating all errors due to convexification.

Thirdly, the total optimization computational time with convexified constraints is comparable with the one without convexification. However, the computational time is significantly high in the cases that a local minimum is found. The computational time is recorded as the elapsed time of the optimization and also averaged over their corresponding numbers of tests. The corresponding numbers of tests are shown in the brackets in the table.

In summary, the convex preservation contributes to a limited amount of extra cost to the total cost and always provides a global minimum with small computational time. Therefore it is concluded that the idea of convexifying the constraint in this problem is more beneficial than disadvantageous in this optimization problem.

2) Sensitivity Validation With Respect to the Optimization Variables: This section observes the optimization variables to illustrate the station distribution of the entire system when the

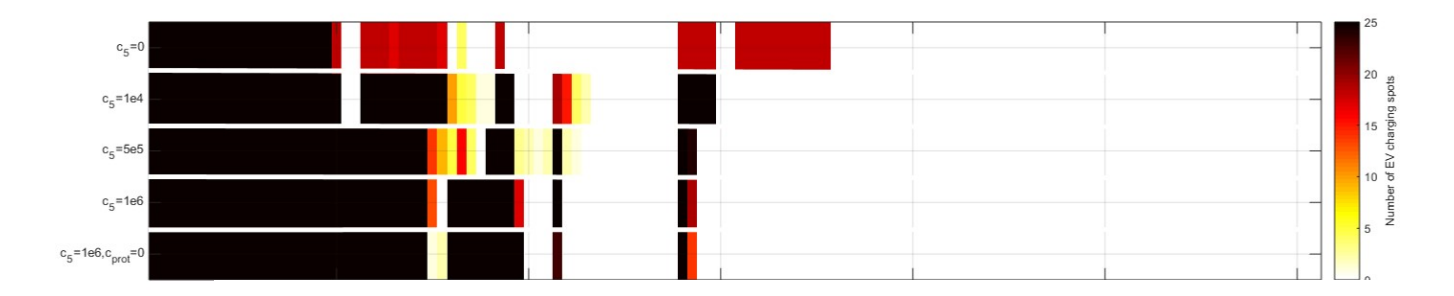


Fig. 6. The station

constraint coefficenclusions upostation in this result the number of the maximum shows the charge

We further for how the constra shown in Fig. 7. representative re distribution due large amount of distribution, the overall character as the constraint

When the vol in the planning, in this case stu 37. As the volta to 5e5, the tota

Fig. 7. The partial topology of the distribution system and the highlight of the area under study.

TABLE V EV charging station placement at bus 33-37 in 123-bus system

Constraint	Constraint coefficient	Placement at bus 33-37
(3), (4), (6)	$c_5 = 0$	0 4 0 0 0
(3), (4), (5), (6)	$c_5 = 1e4$	10 5 4 1 1
(3), (4), (5), (6)	$c_5 = 5e5$	5 16 4 0 25
(3), (4), (5), (6)	$c_5 = 1e6$	25 25 25 25 25
(3), (4), (5)	$c_5 = 1e6$	25 25 25 25 25

bus 33-37 increases from 21 to 50, if we sum up the spot numbers of the second and third data rows in Table V. This actually means when the voltage regulation cost is high, the preferred EV placement location moves to this region. As the voltage regulation coefficient goes higher, each bus in this region reaches its maximum capacity. Furthermore, the last data row in Table V indicates the domination of the voltage regulation constraint does not rely on the existence of the protection constraint.

By observing the overall placement results in the 123-bus system, the following conclusions are drawn:

 The constraint on voltage regulations pushes the EV charging station placement towards the end of the distribution feeder.

 $^2 Adding$  one extra charging spot requires  $15\,\mathrm{m}^2 \sim 20\,\mathrm{m}^2$  land [32], [34], the land use is then around  $375\,\mathrm{m}^2 \sim 500\,\mathrm{m}^2$ . Since more spaces can be provided for non-EVs, this land use range can easily fit into the parking lot design requirements such as the ones in [35].

 $^3$ Given 122 potential stations in the system, theoretically, the maximum station capacity in the whole system is  $122 \times 25 = 3,050$  spots. However, the reality can be that the EV flows per hour have not been saturated to the point that each available station needs to be fitted with a maximum of 25 spots. A 30% capacity indicates  $3,050 \times 0.3 = 915$  spots. It is a feasible scenario for medium voltage distribution network as evidenced in [5], [32].

- The cost derived from the constraint on the protective device is less when the EV charging stations are located near the feeder trunk.
- 3) Sensitivity Validation With Respect to Different Cost Components: In this subsection, we investigate three issues. First of all, how does the amount of EV flow at unit time affect the number of charging stations and total cost? As the number of charges per hour progresses, the number of spots in demand is proportional to the number of EVs per hour, as assumed and governed by (15). As for the number of stations, it reaches its maximum of 122 (assuming no station is built on the slack bus) in Fig. 8a, which is bounded by the electric system capacity constraints (2e) and (2f). Meanwhile, the number of EVs per hour is 6,913. In Fig. 8b, given the EV station capacity of

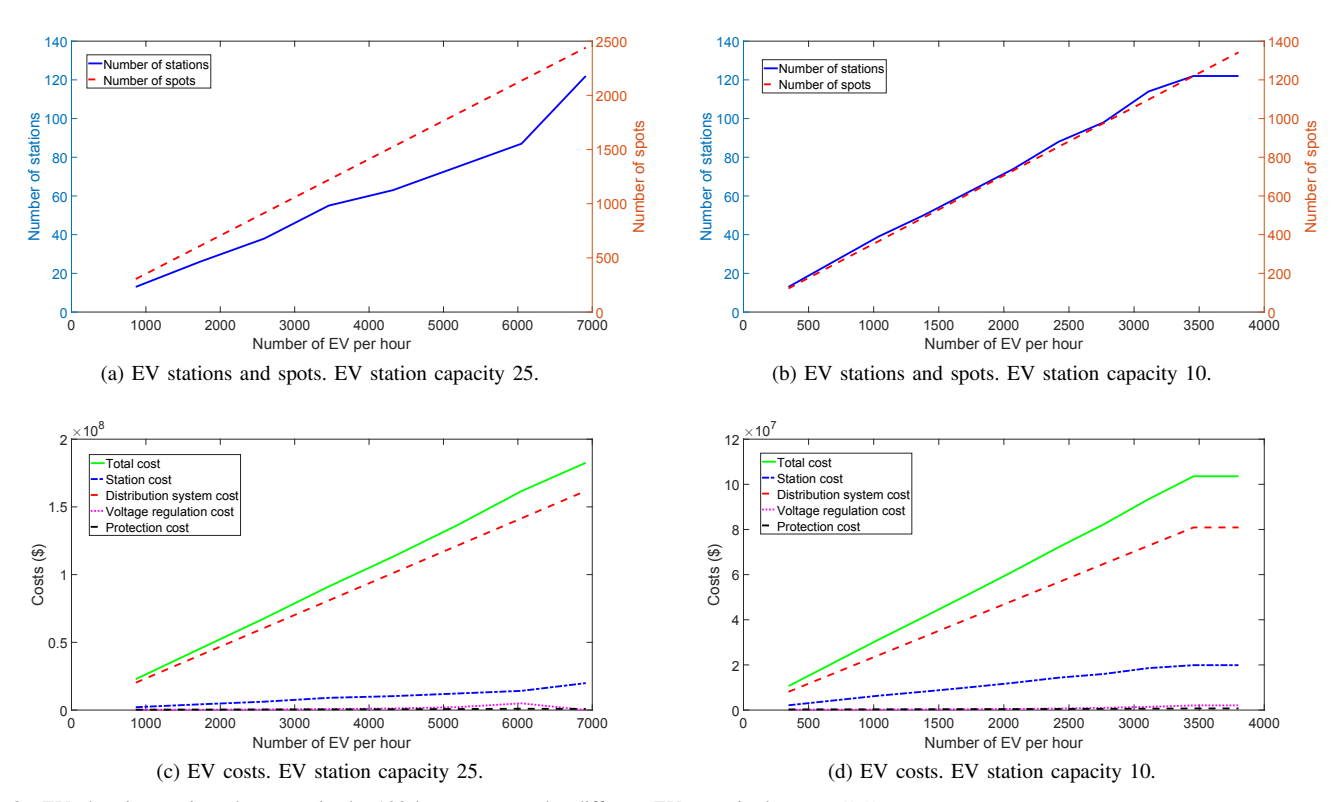


Fig. 8. EV charging station placement in the 123-bus system under different EV magnitude.  $c_5=5e5$ .

10 spots per station, the number of stations saturates at 122 – the maximum number of stations that the current system can hold, when the number of EVs per hour reaches 3,500. The cost diagrams under two EV station capacities are depicted in Fig. 8c and Fig. 8d. The distribution system cost takes up a large portion of the total cost, whereas the costs of voltage regulation and protection upgrade have low cost with the same parameters in Section IV-A.

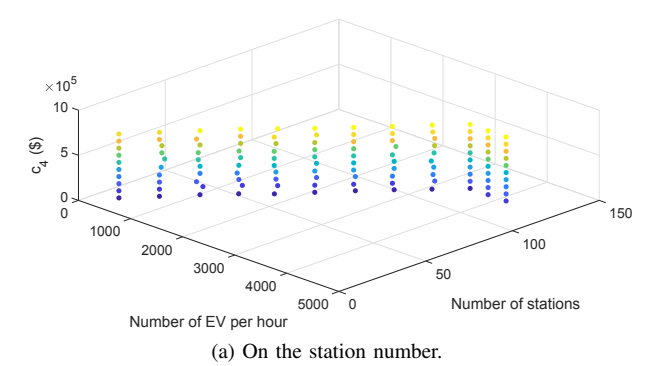
Secondly, what is the effect of distribution expansion cost on the total cost? Due to the labor and land costs in different areas, costs resulting from (3) and (4) varies immensely. Under this circumstance, the effect of the substation expansion coefficient  $c_4$  on the EV charging station placements is investigated and plotted in Fig. 9a and Fig. 9b. From the bottom to top points, the same layers/color represents the same value of  $c_4$ . It can be observed that the number of stations does not rely on the varying of  $c_4$ . The increasing of  $c_4$  does not change the planning of the stations but the total cost. It is easy to see that the larger number of EVs per hour there is, the more  $c_4$  variation alters the total costs.

Thirdly, what are the relations between the amount of EV flow at unit time and the distribution grid operation costs on the voltage regulation and protection upgrade? When the EV charging station cost and distribution expansion cost are not dominantly high, the voltage regulation cost and projection cost affect the total cost. The sensitivity of the voltage regulation cost and projection cost in terms of the number of EVs per hour is presented in Fig. 10. The voltage regulation cost rises quadratically as predicted in Section II-D and cease rising when the number of EVs per hour exceeds the system station capacity, which is 3,500 EVs per hour.

4) Feasibility Analysis: The feasibility of the 123-bus system solutions is evaluated, using the case study the same as in Section IV-C1. The resulting constraint violation  $V_c$  is 7.1953 after averaging the 23 cases that consider different EV flows and station capacity limits. Notably, the constraint violation is mainly contributed by the voltage constraints (2f), which in turn emphasizes the importance of considering the voltage regulation cost (constraint (5)). However, the convexification error of the adopted power flow linearization is small. In the case study, the maximum node voltage difference is  $4.91 \times 10^{-3}$ , obtained by subtracting the estimated solutions with the solutions from the conventional back-forward sweep algorithm. Similar results can be found in [36].

#### D. Results Considering the Economic Parameter Variation

It is also presented here how the optimization variables alter when the economic parameter variation is considered in equation (22). An analysis is applied to the levelized cost coefficients model using the inflation rate of 1%, 2%, and 5%, discount rate of 5%, 7.5%, 10%, and 15%, as well as project time of 1, 5, and 20 years [24]. We have designed five scenarios to show the influence of the economic parameter variation. The first scenario is the same case as in Fig. 8a. where the levelized cost coefficient method is not involved. The second scenarios is the base case for the levelized method, where  $\alpha_1 = 5\%$ ,  $\alpha_2 = \alpha_3 = \alpha_4 = \alpha_5 = 3\%$ ,  $\beta_2 = 15\%$ ,  $\beta_1 = \beta_3 = \beta_4 = \beta_5 = 5\%$ , and T = 20. Scenario 3 is the same as the second scenario except for T=5. Scenario 4 is the same as the second scenario except for  $\alpha_1 = 1\%$ . Scenario 5 is the same as the second scenario except for  $\beta_1 = 15\%$ . The time value of the cost coefficients  $c_{n,i,t}$   $(n = 1, \dots, 5)$  is



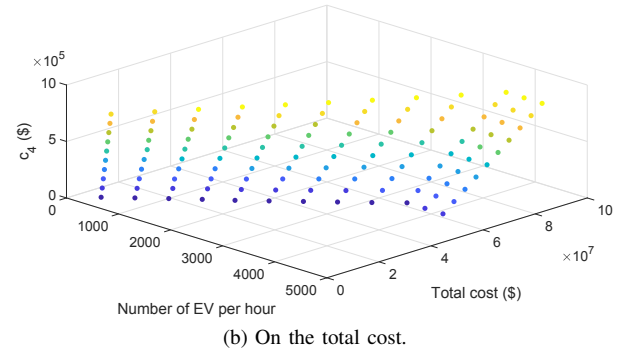


Fig. 9. The effect of the coefficient  $c_4$  on the station number and the total cost.  $c_5 = 5e_5$ . EV station capacity 10.

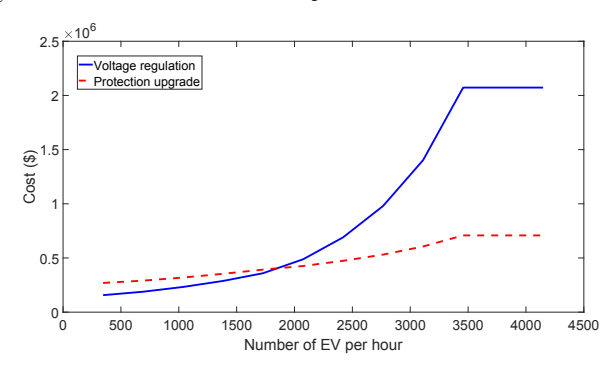


Fig. 10. The sensitivity of the voltage regulation cost and projection cost in terms of the number of EVs per hour.  $c_5=5e5$ . EV station capacity 10.

taken into account as the duration of the project changes. The corresponding results are shown in Fig. 11. It is interesting to see the subtle deviation from the base case affected by the economic parameters as the EV flow increases. For example, scenario 2 and 3 consider the time-sensitive costs given the project time spans of 20 and 5 years. They share at least five crossover points during each level of the EV flows. Behind these two scenarios are two different objective functions that consider the different time value of money.

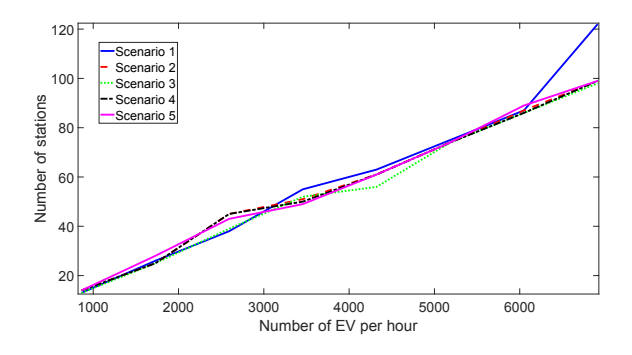


Fig. 11. The number of charging stations under five different scenarios when considering the economic parameter variation.

#### V. DISCUSSIONS

#### A. Applicability in Different Cities and Countries

The formulation of the problem renders itself the flexibility of implementing different types of cost. Due to the variation of costs on land, labor, and equipment in different cities and countries, the coefficient  $c_1$  to  $c_5$  can vary significantly. According to the analysis in Section II-D, the dominating terms are highly dependent on these coefficients. Although the aforementioned costs directly determine the coefficients of constraints (3)-(6), the objective function remains effective in different locations because the objective function aims to minimize the total cost. Actually, in different cities or countries, the dominating constraints might be different.

- Developed countries. Take the States, for example, the labor cost is comparatively high. According to [37], the labor cost takes up to 60% of the EV supply equipment installation cost. That is why the EV charging station and distribution expansion costs are dominantly high.
- Developing countries. We investigate the EV charging station cost for the city of Beijing in China, the corresponding costs are listed, according to [38], as follows (assuming the US Dollar (USD) to Chinese Yuan (CNY) exchange rate is 6.35):  $c_{1,i} = 50,640\,(\$),\,c_{2,i} = 7,122\,(\$),\,c_{3,i} = 43\,(\$/(kVA\cdot km)),\,c_{4,i} = 102\,(\$/kVA)$  It is seen that the EV charging station and distribution expansion costs are much lower compared to the US. The discrepancy in small cities in China is even larger. This phenomenon could eventually make the constraint of voltage regulation the dominant constraint during optimization.

#### B. Results Without Considering the Protection Cost

The cost of protective devices elevates fast when the electric network accommodates more EVs which result in higher steady-state and fault current levels. Consequently, in bigger systems, the cost of the protective devices is altering the EV charging station placement since we are minimizing the total operational cost. Table VI illustrates the EV charging station placement results in two distribution systems under the EV flow of 1,500 per hour with the parameters from Section V-A. It is presented that the protection cost may take up to 8% of the total cost, which cannot be neglected in EV haring station placement planning.

#### VI. CONCLUSIONS

The proposed objective function is ameliorated through the proposed sensitivity analysis and convexification method. The optimization function successfully introduces the costs of distribution expansion, EV station, voltage regulation as

TABLE VI EV charging station placement when the EV flow requires 30% of available spots and the spots limit of each station is 10.

Sys. magnitude	18-bus	115-bus [39]	123-bus [40]
# of stations	6	39	39
# of spots	51	342	366
Total cost (\$)	2.82e6	1.86e7	5.30e6
Percent of prot. cost (\$)	5.89%	8.60%	6.03%

well as a well-designed protective device cost model to this problem. The problem sensitivity is not compromised after the convexification. The idea of the convex preservation of constraints always guarantees a global minimum in different test cases. Meanwhile, the computational time is greatly decreased with convex preservation. Through the numerical results, we realize that the voltage regulation cost is trying to favor the EV charging station placement at the end of branches. However, the protective device upgrade will cost less if more EV charging stations are installed at the main line of the feeder, trying to avoid branch ends. Numerical results also show that the protective device cost is not negligible in the total planning cost. At the end of numerical results, the proposed method illustrates that it is a flexible solution for the EV charging station placement no matter in developed countries or developing countries. To conclude, the proposed method can provide recommendations for the DSOs on future EV charging station planning. Since this work is related to EV charging station planning, future work could incorporate an optimal charging strategy on this determined EV infrastructure.

## APPENDIX A PROTECTIVE DEVICE COSTS

The protective device costs are in Table VII and VIII [21].

TABLE VII
PROTECTIVE DEVICE INSTALLATION AND MAINTENANCE COSTS.

Device type	Install/uninstall cost (\$)	Annual maintenance cost (\$)
Fuse	1,000	50
Recloser	5,000	2,500
Overcurrent relay	1,000	500
DORSR	1,500	750

# Appendix B Nested Logit Model and Charging Demand Estimation

According to [11], the consumer, as a utility maximizer, will always choose the product or service which brings him/her the maximum utility. The utility that the  $w^{th}$  EV owner can obtain from choosing bus node i and service provider k  $(k=1,\cdots,k_{max})$  is defined as  $U^w_{i,k}=\bar{U}^w_{i,k}+\epsilon^w_{i,k}.$  The vector of  $\epsilon^w=[\epsilon^w_{1,1},\cdots,\epsilon^w_{n,1},\epsilon^w_{1,2},\cdots,\epsilon^w_{n,2},\cdots,\epsilon^w_{1,k_{max}},\cdots,\epsilon^w_{n,k_{max}}]^T$  have a generalized extreme value distribution with cumulative distribution function

TABLE VIII
PROTECTIVE DEVICE ACQUISITION COSTS.

Device type	Current (A)	Cost (\$)
	$0 \sim 20$	400
	$21 \sim 50$	700
Fuse	$51 \sim 80$	850
	$81 \sim 100$	1,000
	$101 \sim 200$	1,100
	$0 \sim 50$	15,000
	$51 \sim 100$	19,000
Recloser	$101 \sim 300$	22,000
	$301 \sim 500$	27,000
	$501 \sim 1,000$	30,000
	$0 \sim 50$	4,000
	$51 \sim 100$	4,500
Overcurrent relay	$101 \sim 300$	5,000
	$301 \sim 500$	5,500
	$501\sim1,000$	6,000
	$0 \sim 50$	6,000
	$51 \sim 100$	6,500
DORSR	$101\sim200$	7,000
	$201\sim500$	7,500
	$501\sim1,000$	8,000

$$F(\epsilon^w) = \exp\left(-\sum_{k=1}^{k_{max}} \left(\sum_{i=1}^n e^{-\epsilon_{i,k}^w/\sigma_k}\right)^{\sigma_k}\right), \quad (26)$$

where  $\sigma$  is a measure of the degree of independence. The variable  $\bar{U}^w_{i,k}$  is defined as

$$\bar{U}_{i,k}^w = \bar{W}_k^w + \bar{V}_k^w, \tag{27}$$

$$\bar{W}_k^w = \alpha \frac{1}{t_k} + \beta \frac{p_k}{i_w},\tag{28}$$

$$\bar{V}_{k}^{w} = \mu_{k} d_{i,k}^{w} + \eta_{k} z_{i,k}^{w} + \gamma_{k} r_{i,k}^{w} + \lambda_{k} g_{i,k}^{w} + \delta_{k} m_{i,k}^{w}.$$
 (29)

Concretely,  $t_k$ ,  $p_k$  and  $i_w$  represent the average charging time, the retail charging price, and the income of the  $w^{th}$  EV owner;  $\alpha$ ,  $\beta$  are the corresponding weighting coefficients;  $d^w_{i,k}$  is the deviating distance, which is the route length of this new route minus the route length of the original route;  $z^w_{i,k}$  is the destination indicator, and becomes 1 when the  $i^{th}$  charging station is near the EV owner's travel destination; the vector of  $[r^w_{i,k}, g^w_{i,k}, m^w_{i,k}]^T$  denotes the attractiveness of this charging station in terms of three amenities: restaurant, shopping center, and supermarket, respectively.

The probability that the  $w^{th}$  EV owner will choose the  $i^{th}$  charging station of service provider k is

$$\phi_{i,k}^{w} = \frac{e^{\bar{U}_{i,k}^{w}/\sigma_{k}} \left(\sum_{i=1}^{n} e^{\bar{U}_{i,k}^{w}/\sigma_{k}}\right)^{\sigma_{k}-1}}{\sum_{t=1}^{k_{max}} \left(\sum_{i=1}^{n} e^{\bar{U}_{i,t}^{w}/\sigma_{t}}\right)^{\sigma_{t}}}.$$
 (30)

As for the charging demand estimation, let  $q_w$  ( $w=1,2,\cdots,N_{EV}$ ) denote the total electricity that the  $w^{th}$  EV owner purchases from the charging station ( $N_{EV}$  is the total

number of EVs). The total predicted charging demand of bus node i of service provider k is modeled as:

$$D_{i,k} = \sum_{n=1}^{N_{EV}} q_w \phi_{i,k}^w.$$
 (31)

#### APPENDIX C

#### DERIVATION OF THE AC POWER FLOW LINEARIZATION

Nodal currents can be expressed by the admittance matrix and nodal voltages:

$$\begin{pmatrix} I_S \\ I_N \end{pmatrix} = \begin{pmatrix} Y_{SS} & Y_{SN} \\ Y_{NS} & Y_{NN} \end{pmatrix} \cdot \begin{pmatrix} V_S \\ V_N \end{pmatrix} \tag{32}$$

where S represents the slack node and N is the set of remaining nodes. Each nodal current is related to the voltage by the following ZIP model:

$$I_k = \frac{S_{Pk}^*}{V_k^*} + h \cdot S_{Ik}^* + h^2 \cdot S_{Zk}^* \cdot V_k \tag{33}$$

We linearize the AC power flow equation and express the voltage as a function of the power injected in a closed rectangular form [36]:

$$A + B \cdot V_N^* + C \cdot V_N = 0 \tag{34}$$

with  $A = Y_{NS} \cdot V_S = 2h \cdot S_{PN}^* - h \cdot S_{IN}^*$ ,  $B = h^2 \cdot \operatorname{diag}(S_{PN}^*)$ ,  $C = Y_{NN} - h^2 \cdot \operatorname{diag}(S_{ZN}^*)$ , where  $V_N$  is the vector of non-slack bus voltages,  $S_{ZN}$ ,  $S_{IN}$  and  $S_{PN}$  are the complex power injection of constant impedance load, constant current load and constant power load at non-slack buses,  $h = 1/V_{nom}$ .

From (24), if we neglect high order terms and defining  $V = 1 - \Delta V$ , a linear form is obtained:

$$\frac{1}{V} = \frac{1}{1 - \Delta V} \approx 1 + \Delta V = 2 - V.$$
 (35)

### APPENDIX D

#### IEEE 123-BUS DISTRIBUTION SYSTEM

The single line diagram of the IEEE 123-bus distribution system [40] is shown in Fig. 12.

#### APPENDIX E

#### TRANSPORTATION NETWORK OF SIOUX FALLS

The Sioux Falls network is shown in Fig. 13. Its details can be found in [33].

#### REFERENCES

- [1] S. C. Kuttan. (2016)Creating a level field vehicles Singapore. electric in [Online]. Availfor able: https://www.eco-business.com/opinion/creating-a-level-playingfield-for-electric-vehicles-in-singapore/
- [2] Land Transport Authority, Government of Singapore. (2018) Tax Structure for Cars. [Online]. Available: https://www.lta.gov.sg/content/ltaweb/en/roads-and-motoring/owning-a-vehicle/costs-of-owning-a-vehicle/tax-structure-for-cars.html
- [3] —. (2016) Joint News Release by the Land Transport Authority (LTA) & EDB - Electric Vehicles (EVs) in Every HDB Town by 2020 . [Online]. Available: https://www.lta.gov.sg/apps/news/page.aspx?c=2&id=e030e95da82c-49b4-953c-fc4b3fad7924

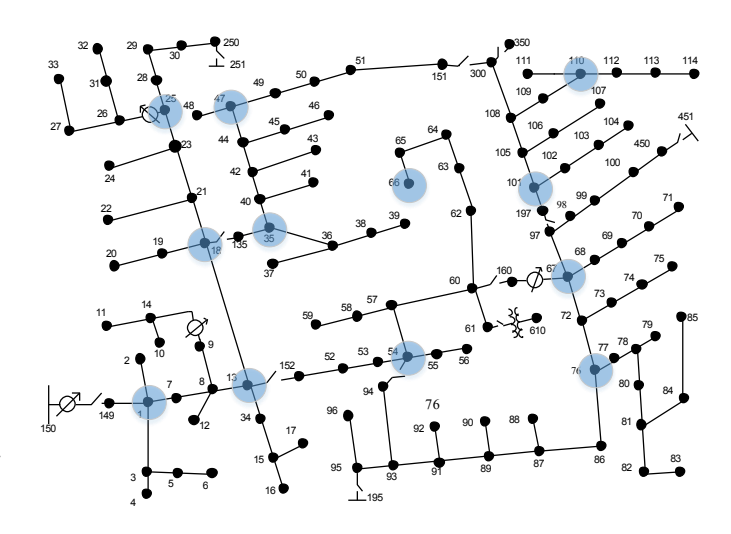


Fig. 12. The single line diagram of the IEEE 123-bus distribution system. The blue circles indicate the direct overlapping with the transportation nodes.

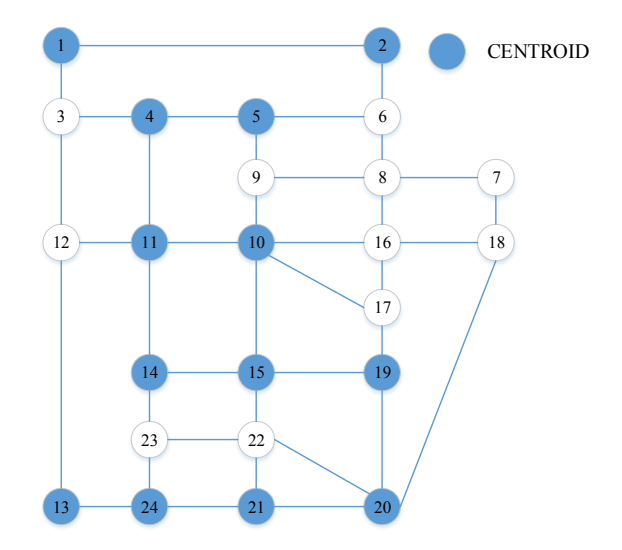


Fig. 13. The benchmark transportation network of Sioux Falls.

- [4] X. Dong, Y. Mu, H. Jia, J. Wu, and X. Yu, "Planning of fast EV charging stations on a round freeway," *IEEE Transactions on Sustainable Energy*, vol. 7, no. 4, pp. 1452–1461, Oct 2016.
- [5] H. Zhang, S. Moura, Z. Hu, and Y. Song, "PEV fast-charging station siting and sizing on coupled transportation and power networks," *IEEE Transactions on Smart Grid*, vol. PP, no. 99, pp. 1–1, 2017.
- [6] X. Wang, C. Yuen, N. U. Hassan, N. An, and W. Wu, "Electric vehicle charging station placement for urban public bus systems," *IEEE Transactions on Intelligent Transportation Systems*, vol. 18, no. 1, pp. 128–139, Jan 2017.
- [7] A. R-Ghahnavieh and P. S-Barzani, "Optimal zonal fast-charging station placement considering urban traffic circulation," *IEEE Transactions on Vehicular Technology*, vol. 66, no. 1, pp. 45–56, Jan 2017.
- [8] Y. Zheng, Z. Y. Dong, Y. Xu, K. Meng, J. H. Zhao, and J. Qiu, "Electric vehicle battery charging/swap stations in distribution systems: Comparison study and optimal planning," *IEEE Transactions on Power Systems*, vol. 29, no. 1, pp. 221–229, Jan 2014.
- [9] R. Mehta, D. Srinivasan, A. M. Khambadkone, J. Yang, and A. Trivedi, "Smart charging strategies for optimal integration of plug-in electric vehicles within existing distribution system infrastructure," *IEEE Transactions on Smart Grid*, vol. 9, no. 1, pp. 299–312, Jan 2018.
- [10] W. Yao, J. Zhao, F. Wen, Z. Dong, Y. Xue, Y. Xu, and K. Meng, "A multi-objective collaborative planning strategy for integrated power distribution and electric vehicle charging systems," *IEEE Transactions* on *Power Systems*, vol. 29, no. 4, pp. 1811–1821, Jul 2014.

- [11] C. Luo, Y. F. Huang, and V. Gupta, "Placement of EV charging stations balancing benefits among multiple entities," *IEEE Transactions on Smart Grid*, vol. 8, no. 2, pp. 759–768, Mar 2017.
- [12] Z. Liu, F. Wen, and G. Ledwich, "Optimal planning of electric-vehicle charging stations in distribution systems," *IEEE Transactions on Power Delivery*, vol. 28, no. 1, pp. 102–110, Jan 2013.
- [13] B. Zhang, Q. Yan, and M. Kezunovic, "Placement of EV charging stations integrated with pv generation and battery storage," in 2017 Twelfth International Conference on Ecological Vehicles and Renewable Energies (EVER), Apr 2017, pp. 1–7.
- [14] K. J. Dyke, N. Schofield, and M. Barnes, "The impact of transport electrification on electrical networks," *IEEE Transactions on Industrial Electronics*, vol. 57, no. 12, pp. 3917–3926, Dec 2010.
- [15] N. Neyestani, M. Y. Damavandi, M. Shafie-Khah, J. Contreras, and J. P. S. Catalo, "Allocation of plug-in vehicles' parking lots in distribution systems considering network-constrained objectives," *IEEE Transactions on Power Systems*, vol. 30, no. 5, pp. 2643–2656, Sept 2015
- [16] A. Y. S. Lam, Y. W. Leung, and X. Chu, "Electric vehicle charging station placement: Formulation, complexity, and solutions," *IEEE Transactions on Smart Grid*, vol. 5, no. 6, pp. 2846–2856, Nov 2014.
  [17] S. Ruifeng, Y. Yang, and K. Y. Lee, "Multi-objective EV charging
- [17] S. Ruifeng, Y. Yang, and K. Y. Lee, "Multi-objective EV charging stations planning based on a two-layer coding spea-ii," in 2017 19th International Conference on Intelligent System Application to Power Systems, Sep 2017, pp. 1–6.
- [18] Y. Xiong, J. Gan, B. An, C. Miao, and A. L. C. Bazzan, "Optimal electric vehicle fast charging station placement based on game theoretical framework," *IEEE Transactions on Intelligent Transportation Systems*, vol. PP, no. 99, pp. 1–12, 2017.
- [19] A. Dukpa, B. Venkatesh, and L. Chang, "Fuzzy stochastic programming method: Capacitor planning in distribution systems with wind generators," *IEEE Transactions on Power Systems*, vol. 26, no. 4, pp. 1971– 1979, Nov 2011.
- [20] N. Kang, J. Wang, R. Singh, and X. Lu, "Interconnection, integration, and interactive impact analysis of microgrids and distribution systems," Argonne National Laboratory (ANL), Tech. Rep., 2017.
- [21] C. Meneses and J. Mantovani, "Improving the grid operation and reliability cost of distribution systems with dispersed generation," *IEEE Transactions on Power Systems*, vol. 28, no. 3, pp. 2485–2496, Aug 2013.
- [22] M. T. Doyle, "Reviewing the impacts of distributed generation on distribution system protection," in *IEEE Power Engineering Society Summer Meeting*, vol. 1, Jul 2002, pp. 103–105.
- [23] D. Karamanis, "Management of moderate wind energy coastal resources," *Energy conversion and management*, vol. 52, no. 7, pp. 2623–2628, 2011.
- [24] C. R. Hallam and C. Contreras, "Evaluation of the levelized cost of energy method for analyzing renewable energy systems: A case study of system equivalency crossover points under varying analysis assumptions," *IEEE Systems Journal*, vol. 9, no. 1, pp. 199–208, 2015.
- [25] M. Sicilia and J. Keppler, "Projected costs of generating electricity," International Energy Agency, Paris, 2010.
- [26] J. A. Taylor and F. S. Hover, "Convex models of distribution system reconfiguration," *IEEE Transactions on Power Systems*, vol. 27, no. 3, pp. 1407–1413, Aug 2012.
- [27] C. Bingane, M. F. Anjos, and S. L. Digabel, "Tight-and-cheap conic relaxation for the ac optimal power flow problem," *IEEE Transactions* on *Power Systems*, vol. 33, no. 6, pp. 7181–7188, Nov 2018.
- [28] J. Agenbroad and B. Holland. (2014) Pulling back the veil on EV charging station costs. [Online]. Available: https://rmi.org/news/pulling-back-veil-ev-charging-station-costs/
- [29] W. Yao, C. Y. Chung, F. Wen, M. Qin, and Y. Xue, "Scenario-based comprehensive expansion planning for distribution systems considering integration of plug-in electric vehicles," *IEEE Transactions on Power Systems*, vol. 31, no. 1, pp. 317–328, Jan 2016.
- [30] U.S. Department of Transportation, Federal Highway Administration. (2009) 2009 National Household Travel Survey. [Online]. Available: http://nhts.ornl.gov
- [31] J. J. Burke, Hard to find information about distribution systems. ABB Power T & D Company, 1999.
- [32] H. Zhang, Z. Hu, Z. Xu, and Y. Song, "An integrated planning framework for different types of PEV charging facilities in urban area," *IEEE Transactions on Smart Grid*, vol. 7, no. 5, pp. 2273–2284, Sep 2016.
- [33] Transportation Networks for Research Core Team, "Transportation networks for research," last accessed 2019-03-05. [Online]. Available: https://github.com/bstabler/TransportationNetworks

- [34] D. Mayfield, "Site design for electric vehicle charging stations, ver. 1.0," Sustainable transportation strategies, 2012.
- [35] University of Houston. (2018) Campus design guidelines and standards. [Online]. Available: http://www.uh.edu/facilitiesservices/departments/fpc/design-guidelines/09\_parking.pdf
- [36] A. Garces, "A linear three-phase load flow for power distribution systems," *IEEE Transactions on Power Systems*, vol. 31, no. 1, pp. 827–828, Jan 2016.
- [37] M. Smith and J. Castellano, "Costs associated with non-residential electric vehicle supply equipment: Factors to consider in the implementation of electric vehicle charging stations," New West Technologies LLC, Colorado, USA., Tech. Rep., Nov 2015.
- [38] Z. Li and M. Ouyang, "The pricing of charging for EVs in China-Dilemma and solution," *Energy*, vol. 36, no. 9, pp. 5765–5778, 2011.
- [39] G. Prettico, F. Gangale, A. Mengolini, A. Lucas, and G. Fulli, "Distribution system operators observatory," *European Commission. Joint Research Centre*, 2016.
- [40] IEEE PES AMPS DSAS Test Feeder Working Group. (2014) 123-node test feeder. [Online]. Available: http://sites.ieee.org/pes-testfeeders/resources/



Qiushi Cui (S'10-M'18) received the M.Sc. degree from Illinois Institute of Technology, and the Ph.D. degree from McGill University, both in Electric Engineering. Currently, he is a postdoctoral scholar of electrical engineering in the Ira A. Fulton Schools of Engineering of Arizona State University (ASU). Prior to joining ASU, he was a research engineer and held a Canada MITACS Accelerate Research Program Fellowship at OPAL-RT Technologies Inc. from 2015 to 2017.

His research interests are in the areas of machine learning and big data applications in power systems, power system protection, smart cities, microgrid, EV integration, renewable energies, and real-time simulation in power engineering. Dr. Cui won the Best Paper Award at the 13<sup>th</sup> IET International Conference in Developments in Power System Protection in Edinburgh, UK, in 2016. He was the winner of the Chunhui Cup Innovation and Entrepreneurship Competition for Overseas Chinese Scholars in Energy Sector in 2018.



Yang Weng (M'14) received the B.E. degree in electrical engineering from Huazhong University of Science and Technology, Wuhan, China; the M.Sc. degree in statistics from the University of Illinois at Chicago, Chicago, IL, USA; and the M.Sc. degree in machine learning of computer science and M.E. and Ph.D. degrees in electrical and computer engineering from Carnegie Mellon University (CMU), Pittsburgh, PA, USA.

After finishing his Ph.D., he joined Stanford University, Stanford, CA, USA, as the TomKat Fellow

for Sustainable Energy. He is currently an Assistant Professor of electrical, computer and energy engineering at Arizona State University (ASU), Tempe, AZ, USA. His research interest is in the interdisciplinary area of power systems, machine learning, and renewable integration.

Dr. Weng received the CMU Deans Graduate Fellowship in 2010, the Best Paper Award at the International Conference on Smart Grid Communication (SGC) in 2012, the first ranking paper of SGC in 2013, Best Papers at the Power and Energy Society General Meeting in 2014, ABB fellowship in 2014, and Golden Best Paper Award at the International Conference on Probabilistic Methods Applied to Power Systems in 2016.



Chin-Woo Tan received the B.S. and Ph.D. degrees in electrical engineering, and the M.A. degree in mathematics from the University of California, Berkeley, CA, USA.

Currently, he is Director of Stanford Smart Grid Lab. He has research and management experience in a wide range of engineering applications intelligent sensing systems, including electric power systems, automated vehicles, intelligent transportation, and supply chain management. His current research focuses on developing data-driven methodologies for

analyzing energy consumption behavior and seeking ways to more efficiently manage consumption and integrate distributed energy resources into grid. Dr. Tan was a Technical Lead for the LADWP Smart Grid Regional Demonstration Project, and a Project Manager with the PATH Program at UC Berkeley for 10 years, working on intelligent transportation systems. Also, he was an Associate Professor with the Electrical Engineering Department at California Baptist University.